Modes of inactivation of trichodiene synthase by a cyclopropane-containing farnesyldiphosphate analog†

Young J. Hong and Dean J. Tantillo*

Received 5th May 2009, Accepted 18th June 2009
First published as an Advance Article on the web 7th August 2009
DOI: 10.1039/b908738a

We describe quantum chemical calculations on the rearrangement of carbocations derived from a cyclopropane-containing analog of farnesyl diphosphate (FPP). These calculations reveal significant differences between the energetics for rearrangement of this analog and FPP itself, suggesting that the behavior of this substrate analog likely does not mirror that of the natural substrate. In addition, our results point to new mechanisms by which this FPP analog inactivates trichodiene synthase.

Introduction

Trichodiene synthase[1] mediates the formation of trichodiene (**1**, Scheme 1), the biosynthetic precursor of the trichothecene antibiotics and mycotoxins,[2] from farnesyl diphosphate (FPP). The widely accepted mechanism for trichodiene formation involves isomerization of (*E*,*E*)-FPP to transoid-nerolidyl diphosphate (transoid-NPP, Scheme 1).[1] Transoid-NPP then undergoes transoid-to-cisoid isomerization, which prepares the substrate for subsequent cyclization. Loss of pyrophosphate and cyclization (either in a concerted or stepwise manner) leads to the bisabolyl cation (**A**), which serves as a key branchpoint in a complex network of reaction pathways leading to a diverse array of sesquiterpenes (*e.g.*, Scheme 1).[3,4] The bisabolyl cation then rearranges to the cuprenyl cation (**E**) *via* a process that is often proposed to proceed *via* putative cation **B**.[1] Two subsequent methyl shifts convert the cuprenyl cation to cation **G**, deprotonation of which produces trichodiene.

While this mechanism (or close relatives) is usually proposed in papers on trichodiene synthase, other pathways involving intermediates **C** or **D** have been proposed as possible alternatives (Scheme 1). Although mechanisms involving both cyclization-then-hydride transfer (**A**→**B**-or-**C**→**E**) and proton transfer-then-cyclization (**A**→**D**→**E**) are consistent with all existing experimental evidence (*e.g.*, tritium labeling of the hydrogen on C6 of FPP),[1,5] quantum chemical calculations have indicated that the proton transfer pathway (Scheme 1) is energetically favored.[6]

FPP analog **2** (Scheme 2) was utilized previously as a mechanism-based inhibitor of trichodiene synthase.[7] Two mechanisms for inactivation by **2** were proposed originally.[7] Compound **2** was designed to react analogously to FPP in the early stages of the trichodiene synthase promoted reaction (compare Schemes 1 and 2), so if cation **B′** was formed in analogy to cation **B**, rearrangement to a reactive cation like **I** was thought to be a possible route to enzyme alkylation. Alternatively, if the reaction of **2** proceeded all the way to cation **F′**, an analog of cation **F**, then a reactive cation like **L** could be formed and alkylate the enzyme. It was hoped that by identifying products of alkylation, additional evidence for the nature of intermediates formed during the trichodiene synthase reaction and the identities of key active site residues could be obtained. When **2** was presented to trichodiene synthase, some inactivation was indeed observed, but the detailed mechanism of inactivation was not determined.[7] Compound **2** also acted as a substrate for trichodiene synthase, being turned over to produce at least three as-yet unidentified hydrocarbon products.[7]

Herein we describe the results of quantum chemical calculations aimed at elucidating the mechanisms by which FPP analog **2** might rearrange and inactivate trichodiene synthase.[8–10] These results also point to additional carbocations that could be the ultimate precursors of the products formed from **2** by trichodiene synthase.

Methods

All calculations were performed with GAUSSIAN03.[11] All geometries were optimized using the B3LYP/6–31+G(d,p) method.[12] All stationary points were characterized by frequency calculations and reported energies include zero-point energy corrections (unscaled). Intrinsic reaction coordinate (IRC) calculations were used for further characterization of all transition state structures.[13] The B3LYP method is known to perform reasonably well in the prediction of geometries and behavior of carbocations.[4,6,8,14] To address the reported tendency of the B3LYP method to underestimate reaction energies for hydrocarbon cyclization reactions,[15] we also calculated mPW1PW91/6–31+G(d,p)//B3LYP/6–31+G(d,p) energies. These energies include unscaled zero-point energy corrections from B3LYP/6–31+G(d,p) frequency calculations. We have used these methods previously in studies of other terpene-forming carbocation rearrangement reactions.[4,6,8] All energies for intermediates and transition state structures in this report are

Department of Chemistry, University of California, Davis, One Shields Avenue, Davis, CA 95616, USA. E-mail: tantillo@chem.ucdavis.edu

† Electronic supplementary information (ESI) available: Coordinates and energies for all computed structures, along with full Gaussian citation and IRC plots, as well as details on calculations at other levels of theory. See DOI: 10.1039/b908738a

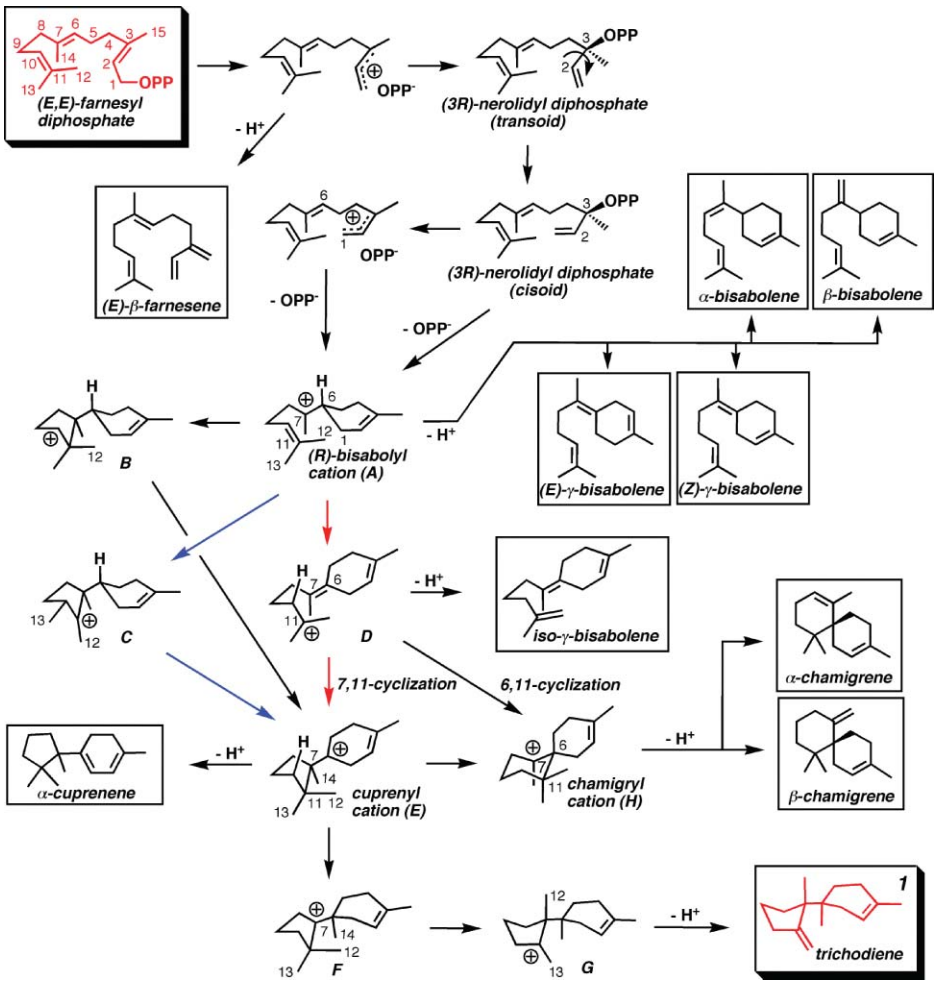

Scheme 1

relative to that of **A1** or **A1′** (Fig. 1 and 3), whose energies are set to [0.00] kcal/mol. Occasionally, the energies of transition state structures were slightly lower than those of attached minima after zero point energy corrections were added to each or single point energies at a level of theory different than that used for geometry optimization were calculated for the structures in question. This situation is not uncommon for flat surfaces and, in fact, reinforces just how flat some of the regions of the considered potential energy surfaces are. Free energies (B3LYP/6–31+G(d,p)), single point energies using the MPWB1K functional, and solvation calculations (CPCM(UAKS) in benzene) are described in the ESI;† the conclusions described in the text are not changed significantly when these alternative energies are considered. Structural drawings were produced using Ball & Stick.[16] Atom numbering is shown for FPP and FPP analog **2** in Schemes 1 and 2.

Results and discussion

The conversion of the bisabolyl cation (**A**) to the cuprenyl cation (**E**) involves two key processes, a hydrogen transfer step and a cyclization step, which differ in their order for the proton (**A**→**D**→**E**) and hydride (**A**→**B**-or-**C**→**E**) transfer mechanisms (Scheme 1). We have now examined analogous pathways for bisabolyl cation analog **A′** (Scheme 2).

Proton transfer pathways

The first step in the proton transfer mechanism is an intramolecular proton transfer from C6 to C10, which converts bisabolyl cation analog **A′** (here, specifically conformer **A1′**) into **D′** (Fig. 1a). This conversion is associated with a computed energy barrier of ~8–10 kcal/mol and is endothermic by ~9–10 kcal/mol (Fig. 1a and 2a). This barrier is comparable to, but slightly higher than, that for the corresponding bisabolyl cation conformer **A1** (Fig. 3a and 4a).[6] Cation **D′** can then undergo 7,11-cyclization (without having to change its conformation) to form **E1′**. The transition state structure for this conversion is ~16–17 kcal/mol higher in energy than **A1′** (Fig. 1a and 2a). It is notable that this process is significantly more difficult than the analogous process for the normal substrate (Fig. 3a and 4a), presumably due in large part to the strain associated with forming a

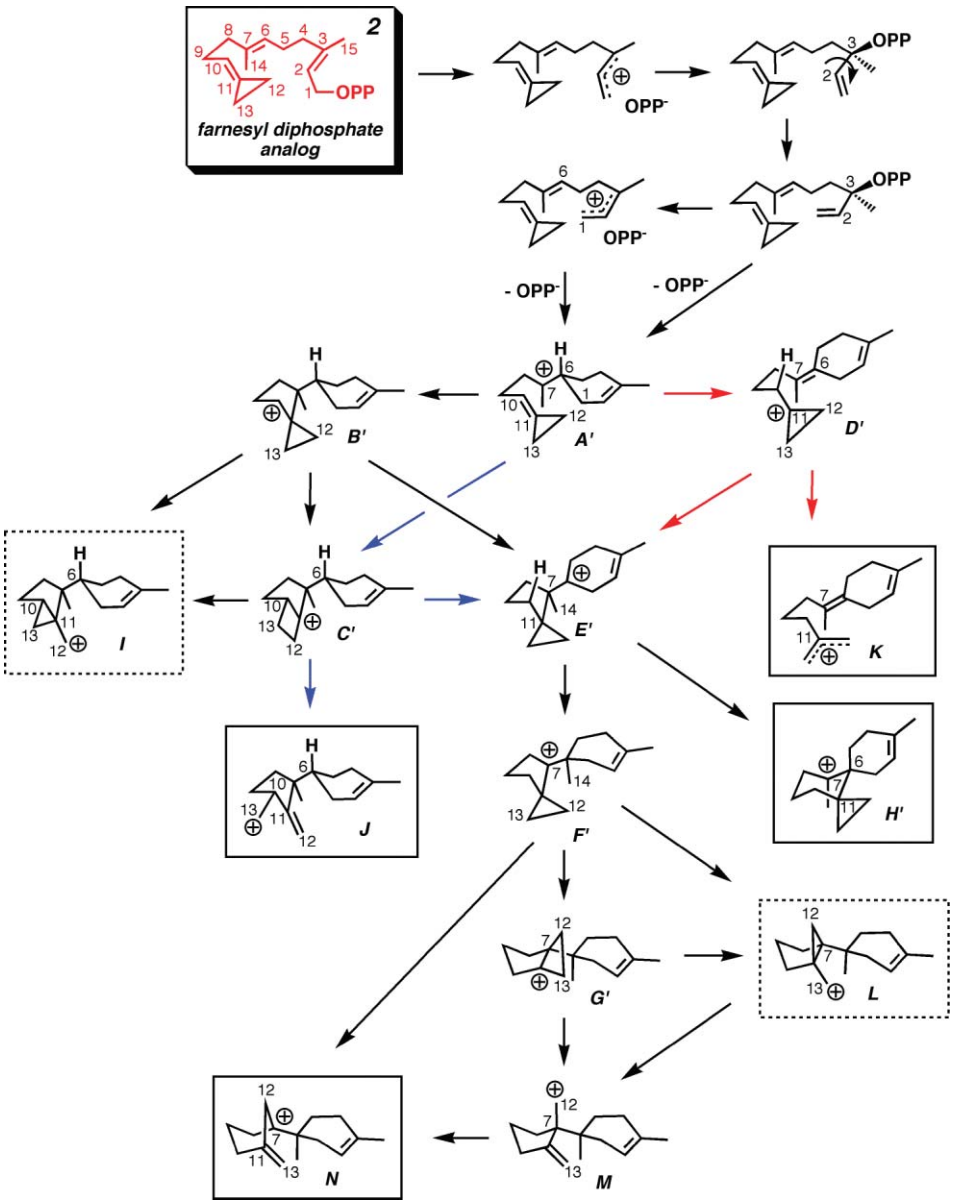

Scheme 2

spiro-connected cyclopropane. Cuprenyl cation analog **E1′** is expected to then undergo a methyl shift, however conformer **E1′** is not productive for this rearrangement. Conformer **E3′**, which is ~8–9 kcal/mol higher in energy than conformer **E1′**, is, and these two conformers are connected by a third, **E2′** (Fig. 1a). Methyl shift of **E3′** leads to cation **F′**. The next expected conversion is a ring-expanding 1,2-alkyl shift that corresponds to the methyl shift that converts **F** to **G** in the reaction of **A1**. However, we were unable to find the expected cation **G′**. Instead we located a transition state structure (Fig. 1a) that appeared initially to be the transition structure for the subsequent **G′→M** reaction shown in Scheme 2. However, IRC calculations indicate that this transition state structure actually connects **F′** directly to cation **N**. The **F′→N** interconversion is a concerted reaction in which three events—alkyl (C12) shifting, 12,13-bond breaking, and alkyl (C11) shifting—occur asynchronously (Fig. 5).[9] This sequence of events is illustrated in Scheme 3; it is important to note, however, that the two structures enclosed in brackets are *not* discrete minima on the potential energy surface. Overall, the **A1′→N** pathway has a significantly higher barrier than does the **A1→G** pathway and is significantly more exothermic (Fig. 2a and 4a).

Along this pathway, a cyclopropyl cation, **D′**, is encountered. Cyclopropyl cations are notoriously unstable towards electrocyclic ring-opening to form allylic cations,[17] and are often not even found as discrete intermediates.[17,18] Ring-opening of **D′** to form

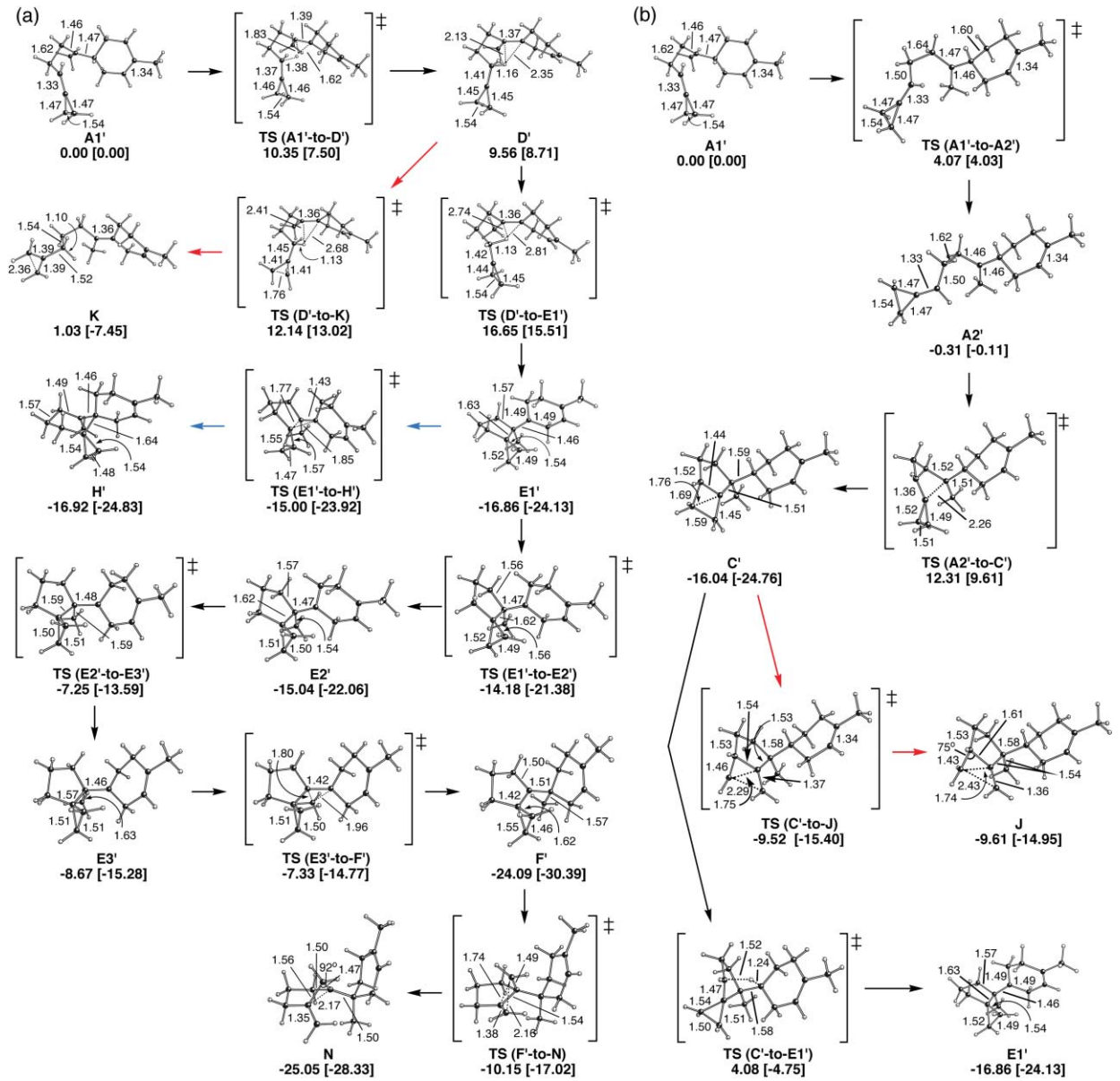

Fig. 1 Computed rearrangement of bisabolyl cation analog **A′**: (a) the proton transfer pathway, (b) the hydride transfer pathway. Computed structures (distances in Å) and energies (in kcal/mol) of intermediates and transition structures are shown: B3LYP/6–31+G(d,p)//B3LYP/6–31+G(d,p) in normal type and mPW1PW91/6–31+G(d,p)//B3LYP/6–31+G(d,p) in brackets.

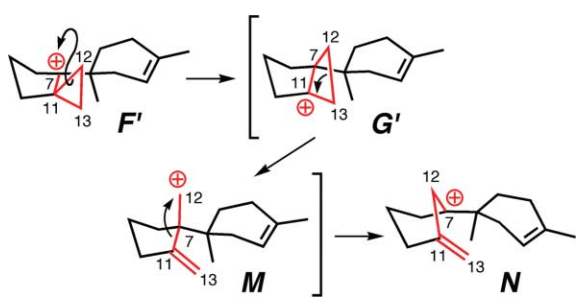

Scheme 3

K (Scheme 2 and Fig. 1a) does indeed have only a small barrier (~3–5 kcal/mol) and the ring-opening transition state structure is ~2–5 kcal/mol lower in energy than **TS (D′→E1′)** (Fig. 1a and 2a). We also explored a potential alternative rearrangement of cation **E1′**. Ring expansion of **E1′** to form **H′** (Scheme 2 and Fig. 1a) also has only a small barrier, one that is significantly lower than that for the conversion of **E1′** to **F′**. These results suggest that such ring-opening or ring-expansion reactions could be routes to cations that inactivate trichodiene synthase and/or precede the as-yet unidentified hydrocarbons produced from **2** (*vide supra*).[7]

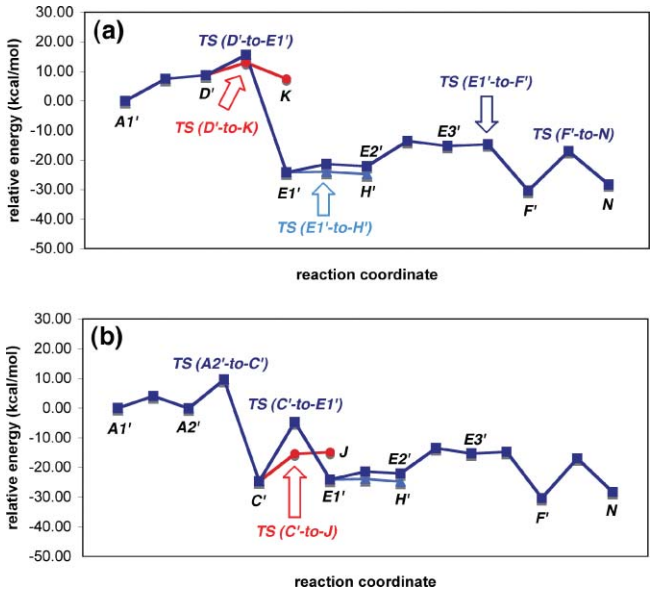

Fig. 2 Overall energetics (mPW1PW91/6–31+G(d,p)//B3LYP/6–31+G(d,p)) for the rearrangement of the bisabolyl cation analog **A′**: (a) the proton transfer pathway, (b) the hydride transfer pathway.

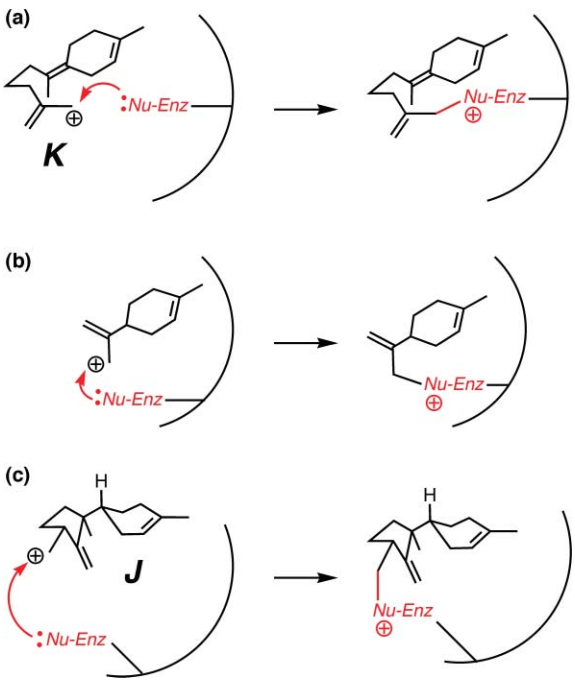

Scheme 4

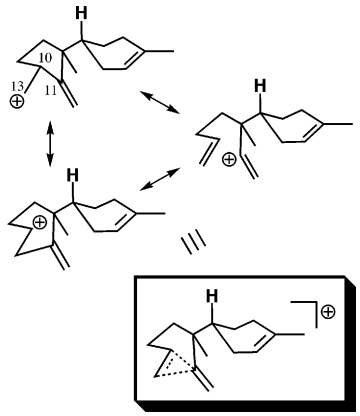

Chart 1

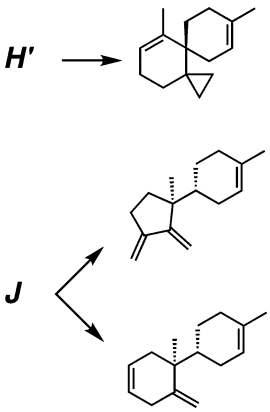

Scheme 5

Hydride transfer pathways

Structures involved in the hydride transfer mechanism for rearrangement of **2**, along with their computed relative energies, are shown in Fig. 1b and 2b. We were able to locate a transition state structure with the expected geometry for the formation of the hypothetical cation **B′** *via* cation–alkene cyclization. However, we were unable to locate a minimum corresponding to cation **B′** itself. Instead we found a minimum corresponding to tertiary cation **C′** (Scheme 2 and Fig. 1b). IRC calculations indicate that the transition state structure is actually connected directly to **C′** and the production of this cation from **A2′** involves concerted but very asynchronous cyclization and alkyl shifting (C10-to-C11) events (Fig. 6, left).[6,9] In the structure of **C′**, the C10–C11 σ-bond is only 1.44 Å long, while the C10–C13 σ-bond is elongated to 1.69 Å, consistent with strong hyperconjugation of the C10–C13 σ-bond with cationic center C11. Moreover, the C11–C12 σ-bond is only 1.45 Å long, the C12–C13 σ-bond is slightly elongated to 1.59 Å, and the distance between C11 and C13 is also quite short (1.76 Å). These structural features are not unusual for nonclassical cations of this type, which are often described as bicyclobutonium ions.[19]

A transition state structure that connects **C′** directly to the cuprenyl cation analog **E1′** through concerted but asynchronous alkyl shift (back in the opposite direction) and hydride transfer events was also located (Fig. 1b and 6, right). The **A2′→C′→E1′** transformation is analogous to the "temporary methyl shift"

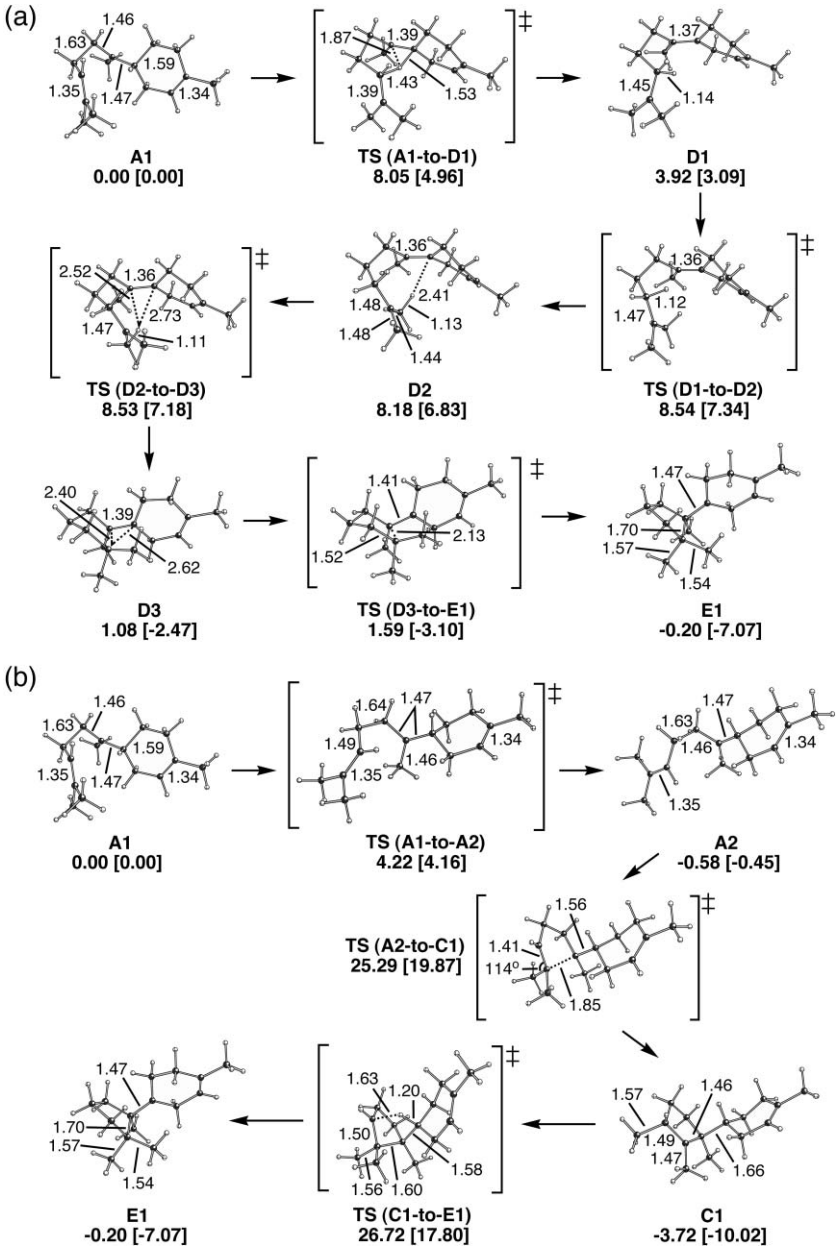

Fig. 3 Computed rearrangement of the bisabolyl cation (**A**): (a) the proton transfer pathway, (b) the hydride transfer pathway. Computed structures (distances in Å) and energies (in kcal/mol) of intermediates and transition structures are shown: B3LYP/6–31+G(d,p)//B3LYP/6–31+G(d,p) in normal type and mPW1PW91/6–31+G(d,p)//B3LYP/6–31+G(d,p) in brackets.

observed in the rearrangement of bisabolyl cation **A2** (Fig. 3b).[6,9] These rearrangements allow both systems to avoid the formation of secondary carbocations.[4] As shown in Fig. 1b, 2b, 3b, and 4b, the energy barrier associated with the cyclization of **A2′** is much less for the cyclopropane-containing system, likely due in large part to the relief of strain and development of (nonclassical) delocalization associated with the ring expansion that accompanies cyclization. Thus, unlike with FPP, analog **2** may well rearrange *via* hydride transfer rather than proton transfer. Note also that **C′** is kinetically stable, as it appears to be trapped between two large energy barriers, suggesting that **C′** could be the ultimate precursor of products derived from **2**.

As mentioned above, cyclopropylcarbinyl cation **I** was proposed as a possible enzyme alkylator in the original report on **2**.[7] While we were not able to locate a minimum corresponding to **I**, we found a transition state structure that connects **C′** to cation **J** (Fig. 1b). Although this cation is formally primary, C11 is actually bridging between C10 and C13; in other words, **J** is also a nonclassical cation (Chart 1; **J** appears to reside in a relatively flat region

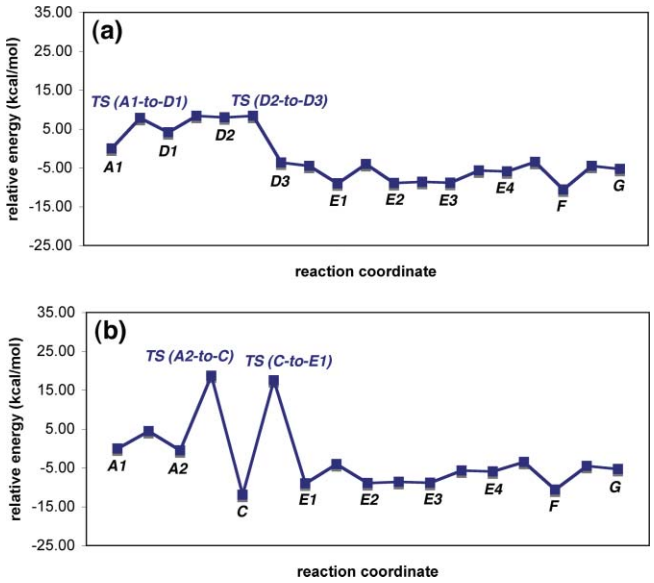

Fig. 4 Overall energetics (mPW1PW91/6–31+G(d,p)//B3LYP/6–31+G(d,p)) for the rearrangement of the bisabolyl cation: (a) the proton transfer pathway, (b) the hydride transfer pathway.

of the potential energy surface, however).[19] Note that this cation forms more readily than does **E1′** (*i.e.*, **TS (C′-to-J)** is significantly lower in energy than **TS (C′-to-E1′)**; Fig. 1b and 2b).

Implications

The results described above lead us to several predictions. Overall, the reactivity of FPP analog **2** is likely significantly different from that of FPP itself. Whereas for FPP a proton transfer mechanism for formation of the cuprenyl cation is strongly preferred on energetic grounds (Fig. 3 and 4),[6] a hydride transfer mechanism is actually preferred for analog **2** (Fig. 1 and 2). For both the hydride and proton transfer pathways for **2**, diversions that occur before **E′** is formed, which lead to cations different than those proposed originally, seem likely. If a proton transfer path is followed, then intermediate **D′** is more likely to open to allylic cation **K** than to continue on to **E1′** (Scheme 2, Fig. 1a and 2a). Cation **K** could then be attacked by the enzyme (in the active site or outside)[20] to form a covalent adduct that is responsible for inactivation (Scheme 4a); irreversible inactivation *via* alkylation by an allylic carbocation has also been proposed for a cyclopropane-containing geranyl diphosphate analog that reacts with pinene synthase (Scheme 4b).[21] If a hydride transfer pathway is followed, formation of cation **J** seems likely (Scheme 2, Fig. 1b and 2b, Chart 1). This cation could also alkylate the enzyme, leading to inactivation (Scheme 4c; other sites of attack are also possible) or could be deprotonated leading to one of the hydrocarbon products observed to be formed (but not yet identified) from trichodiene synthase (*e.g.*, Scheme 5).[7] If cation **E1′** is actually formed (by either a proton or hydride transfer path), then we predict that cation **H′** could form as well (Scheme 2, Fig. 1a and 2a,b). This cation could also alkylate the enzyme or could lead to hydrocarbon products upon deprotonation (*e.g.*, Scheme 5). The other cations shown in Scheme 2 could also behave as alkylators

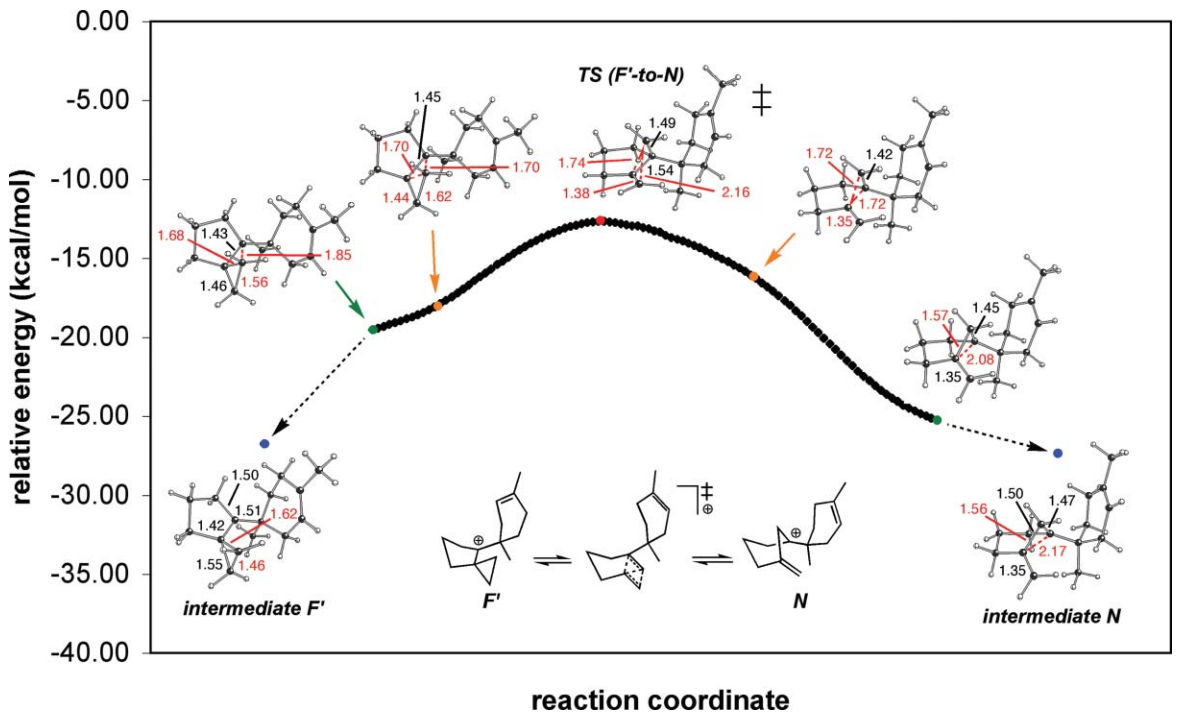

Fig. 5 Conversion of **F′** to **N** based on IRC calculations.

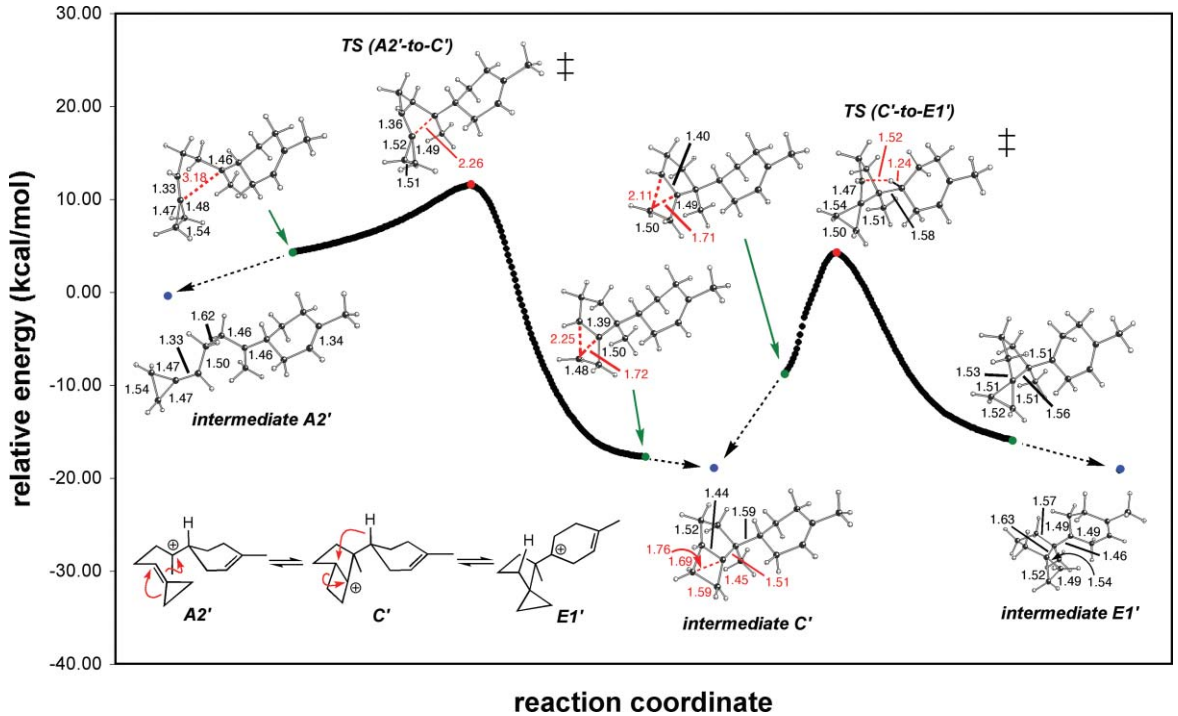

Fig. 6 Conversion of the bisabolyl cation analog **A2′** to **E1′** *via* **C′** based on IRC calculations.

or be deprotonated, but this reactivity could have been expected prior to our theoretical work.

Acknowledgements

We gratefully acknowledge UC Davis, the National Science Foundation's CAREER program, and the National Science Foundation's Partnership for Advanced Computational Infrastructure (Pittsburgh Supercomputer Center) for support. We thank Mike Lodewyk and David Cane for helpful comments.

References

1 M. J. Rynkiewicz, D. E. Cane and D. W. Christianson, *Proc. Natl. Acad. Sci. U. S. A.*, 2001, **98**, 13543–13548; D. E. Cane, H. T. Chiu, P. H. Liang and K. S. Anderson, *Biochemistry*, 1997, **36**, 8332–8339; M. J. Rynkiewicz, D. E. Cane and D. W. Christianson, *Biochemistry*, 2002, **41**, 1732–1741; L. S. Vedula, J. Jiang, T. Zakharian, D. E. Cane and D. W. Christianson, *Arch. Biochem. Biophys.*, 2008, **469**, 184–194; L. S. Vedula, Y. Zhao, R. M. Coates, T. Koyama, D. E. Cane and D. W. Christianson, *Arch. Biochem. Biophys.*, 2007, **466**, 260–266.

2 J. R. Hanson and P. M. Adams, *Chem. Commun.*, 1970, 1569–1570; B. Achilladelis, P. M. Adams and J. R. Hanson, *Chem. Commun.*, 1970, 511; R. W. J. Wannemacher and S. L. Wiener, "Trichothecene Mycotoxins" in *Medical Aspects of Chemical and Biological Warfare*, ed. F. R. Sidell, E. T. Takafuji and D. R. Franz, Office of the Surgeon General, Walter Reed Army Medical Center, Washington, DC. 1997, Ch. 34; A. E. Desjardins, *J, Agric. Food Chem.*, 2009, **57**, 4478–4484.

3 P. M. Dewick, *Nat. Prod. Rep.*, 2002, **19**, 181–222; W. Parker, J. S. Roberts and R. Ramage, *Q. Rev. Chem. Soc.*, 1967, **21**, 331–363; D. E. Cane, *Chem. Rev.*, 1990, **90**, 1089–1103; L. G. Cool, *Phytochemistry*, 2005, **66**, 249–260; C. G. Jones, E. L. Ghisalberti, J. A. Plummer and E. L. Barbour, *Phytochemistry*, 2006, **67**, 2463–2468; P. Mercke, J. Crock, R. Croteau and P. E. Brodelius, *Arch. Biochem. Biophys.*, 1999, **369**, 213–222; S. Wu, M. A. Schoenbeck, B. T. Greenhagen, S. Takahashi, S. Lee, R. M. Coates and J. Chappell, *Plant Physiol.*, 2005, **138**, 1322–1333.

4 Y. J. Hong and D. J. Tantillo, *J. Am. Chem. Soc.*, 2009, **131**, 7999–8015.

5 D. Arigoni, D. E. Cane, B. Müller and C. Tamm, *Helv. Chim. Acta*, 1973, **56**, 2946–2949.

6 Y. J. Hong and D. J. Tantillo, *Org. Lett.*, 2006, **8**, 4601–4604.

7 D. E. Cane and T. E. Bowser, *Bioorg. Med. Chem. Lett.*, 1999, **9**, 1127–1132.

8 This report is part 6 in our "Theoretical Studies on Farnesyl Cation Cyclization" series. For parts 1–5, see refs. 4, 6, and: M. W. Lodewyk, P. G. Gutta and D. J. Tantillo, *J. Org. Chem.*, 2008, **73**, 6570–6579; P. Gutta and D. J. Tantillo, *J. Am. Chem. Soc.*, 2006, **128**, 6172–6179; S. C. Wang and D. J. Tantillo, *Org. Lett.*, 2008, **10**, 4827–4830. For computational work on related biosynthetic and biomimetic carbocation reactions, see refs. 9 and 10.

9 D. J. Tantillo, *J. Phys. Org. Chem.*, 2008, **21**, 561–570.

10 Y. J. Hong and D. J. Tantillo, *Nature Chemistry*, 2009, **1**, 384–389; G. A. Ho, D. H. Nouri and D. J. Tantillo, *Tetrahedron Lett.*, 2009, **50**, 1578–1581; P. Gutta and D. J. Tantillo, *Org. Lett.*, 2007, **9**, 1069–1071; D. Willenbring and D. J. Tantillo, *Russ. J. Gen. Chem.*, 2007, **51**, 49–55; G. A. Ho, D. H. Nouri and D. J. Tantillo, *J. Org. Chem.*, 2005, **70**, 5139–5143; D. H. Nouri and D. J. Tantillo, *Curr. Org. Chem.*, 2006, **10**, 2055–2074. For leading references on related computational work, see: B. A. Hess, *J. Am. Chem. Soc.*, 2002, **124**, 10286–10287; B. A. Hess, *Org. Lett.*, 2003, **5**, 165–167; B. A. Hess and L. Smentek, *Org. Lett.*, 2004, **6**, 1717–1720.

11 M. J. Frisch *et al.*, *Gaussian03, revision D.01*, Gaussian, Inc. Pittsburgh, PA, 2003 (full reference in ESI).

12 A. D. Becke, *J. Chem. Phys.*, 1993, **98**, 5648–5652; A. D. Becke, *J. Chem. Phys.*, 1993, **98**, 1372–1377; C. Lee, W. Yang and R. G. Parr, *Phys. Rev. B*, 1988, **37**, 785–789; P. J. Stephens, F. J. Devlin, C. F. Chabalowski and M. J. Frisch, *J. Phys. Chem.*, 1994, **98**, 11623–11627.

13 C. Gonzalez and H. B. Schlegel, *J. Phys. Chem.*, 1990, **94**, 5523–5527; K. Fukui, *Acc. Chem. Res.*, 1981, **14**, 363–368.

14 Y. J. Hong and D. J. Tantillo, *J. Org. Chem.*, 2007, **72**, 8877–8881; P. Gutta and D. J. Tantillo, *Angew. Chem., Int. Ed.*, 2005, **44**, 2719–2723; M. D. Bojin and D. J. Tantillo, *J. Phys. Chem. A*, 2006, **110**, 4810–4816.

15 S. P. T. Matsuda, W. K. Wilson and Q. Xiong, *Org. Biomol. Chem.*, 2006, **4**, 530–543.

16 N. Müller, A. Falk and G. Gsaller, *Ball & Stick V.4.0a12, molecular graphics application for MacOS computers*, Johannes Kepler University, Linz, 2004.

17 G. K. S. Prakash, H. Buchholz, V. P. Reddy, A. de Meijere and G. A. Olah, *J. Am. Chem. Soc.*, 1992, **114**, 1097–1098.
18 For leading references on cyclopropyl cations, see: D. H. Nouri and D. J. Tantillo, *J. Org. Chem.*, 2006, **71**, 3686–3695; E. C. Friedrich, in *The Chemistry of the Cyclopropyl Group*, ed. Z. Rappoport, Wiley, New York, 1987; G. Boche and H. M. Walborsky, in *Cyclopropane Derived Reactive Intermediates*, ed. S. Patai and Z. Rappoport, Wiley, Chichester, 1990, Ch. 3; E. N. Marvell, in *Thermal Electrocyclic Reactions*, Academic Press, New York, 1980, Ch. 3; L. Radom, P. C. Hariharan, J. A. Pople and P. v. R. Schleyer, *J. Am. Chem. Soc.*, 1973, **95**, 6531–6544; S. I. Kozhushkov, T. Späth, M. Kosa, Y. Apeloig, D. S. Yufit and A. de Meijere, *Eur. J. Org. Chem.*, **2003**, 4234–4242.
19 For leading references on bicyclobutonium cations, see: M. Saunders and H. U. Siehl, *J. Am. Chem. Soc.*, 1980, **102**, 6868–6869; M. Saunders, K. E. Laidig, K. B. Wiberg and P. v. R. Schleyer, *J. Am. Chem. Soc.*, 1988, **110**, 7652–7659; W. Koch, B. Liu and D. J. DeFrees, *J. Am. Chem. Soc.*, 1988, **110**, 7325–7328; J. S. Staral, I. Yavari, J. D. Roberts, G. K. S. Prakash, D. J. Donovan and G. A. Olah, *J. Am. Chem. Soc.*, 1978, **100**, 8016–8018; P. C. Myhre, G. G. Webb and C. S. Yannoni, *J. Am. Chem. Soc.*, 1990, **112**, 8992–8994. For leading references on nonclassical cations, see: Issue 12 of *Acc. Chem. Res.*, 1983, **16**; H. C. Brown, in *The Nonclassical Ion Problem*, Plenum Press, New York. 1977; G. A. Olah, K. K. Laali, Q. Wang and S. G. K. Prakash, in *Onium Ions*, Wiley-Interscience, New York, 1998.
20 D. E. Cane, personal communication.
21 P. McGeady and R. Croteau, *Arch. Biochem. Biophys.*, 1995, **317**, 149–155R. Croteau, W. R. Alonso, A. E. Koepp, J. H. Shim and D. E. Cane, *Arch. Biochem. Biophys.*, 1993, **307**, 397–404.